Trace ions rejection tunning in NF by selecting solution composition: ion permeances estimation

Neus Pagès[a], Mònica Reig[a], Oriol Gibert[a,b], José Luis Cortina[a,b,*]

[a]*Chemical Engineering Department, Universitat Politècnica de Catalunya UPC-BarcelonaTECH*

Av. Diagonal 647, E-08028 Barcelona, Spain

[b]*Water Technology Center CETaqua*

Carretera d'Esplugues 75, E-08940 Cornellà de Llobregat, Spain

[*]*jose.luis.cortina@upc.edu*

Abstract

Nanofiltration (NF) is suggested to selectively remove ionic species in aqueous process streams taking benefit of both membrane and aqueous solution composition. The importance of predicting and optimizing selective ion rejections by NF not only of major compounds (e.g. NaCl, Na_2SO_4, $MgCl_2$, $MgSO_4$) but also of minor ones such as ammonium (NH_4^+), nitrate (NO_3^-), bromide (Br^-), iodide (I^-) typically present in natural and industrial process streams is crucial. The current work explores ion rejection patterns and membrane ion permeances using the phenomenological Solution-Electro-Diffusion-Film (SEDF) model. It makes possible rapid calculations that account for the effects of spontaneously arising electric fields on rejections. Experimental ion rejection data of several inorganic ions species at various transmembrane pressures and at fixed cross-flow velocity have been obtained with NF270 membrane. A number of trace ions (Na^+, K^+, Cl^-, Ca^{2+}, Mg^{2+}, SO_4^{2-}, NO_3^-, NH_4^+, Br^- and I^-) have been used in combination with various dominant salts (NaCl, $MgCl_2$, $MgSO_4$) as model feed solutions. Results showed that dominant salts were moderately (NaCl) and highly ($MgCl_2$, $MgSO_4$) rejected when some ions are divalent, while trace ions exhibited quite variable rejection, including negative ones mainly at low transmembrane volume flows. The electric field of membrane potential can accelerate or retard the ion flows to the permeate, so negative or unexpectedly high rejections could be observed. Ions transport was shown to be affected by the membrane chemistry (e.g. acid-base properties of the un-crosslinked carboxylic and amine groups) and the dielectric exclusion phenomena. From the modelling procedure, ionic membrane permeances were determined for various multi-ion systems studied. Results showed that nature of dominant salt composition can be used to control the rejection of minor components.

Keywords

Nanofiltration; cross-flow filtration; electrolytes mixture; ion rejections; solution-electro-diffusion-film model; ion membrane permeance.

1. INTRODUCTION

Nanofiltration (NF) is a new technological solution for the removal of both major and minor organic and inorganic compounds from aqueous solutions [1–3]. In comparison with reverse osmosis (RO), NF needs less pressure to provide the same volume flow (but usually with lower quality) and offers higher ion selectivities. Typically, NF are thin-film composites -made from various polymers such as (aromatic) polyamides, polysulfone/poly(ether sulfone)/sulfonated polysulfone, polyimide and poly(piperazine amide) [4]. Like RO, NF membranes contain functional groups (not fully cross-linked carboxylic and amine groups), resulting from the synthesis, that can be charged, depending on the pH of the solution in contact with the membrane. At neutral pH, NF membranes are usually slightly negatively charged (e.g. due to deprotonation of the carboxylic groups) as their isoelectric points are around pH 3–4.5 [5–10]. However, determining the chemical membrane composition, in terms of free functional groups, is still an important challenge especially in view of explaining the different ion rejections occurring with various kinds of NF membranes [7,11–13]. Multi-ionic solutions occur in virtually all practical applications of membrane processes, and the solution composition, in terms of chemical nature of the ions, especially in terms of charge (sign and magnitude) and the relative molar compositions, has been demonstrated to play a critical role. Rejection of a given ion depends not only on ion properties, but also on the solution environment (other ions present). As an example, recently, Umpuch et al. [14], investigated how the addition of strong electrolytes (e.g. NaCl or Na_2SO_4) affected the selectivity of the sodium lactate/glucose separation by NF. The addition of Na_2SO_4 (0.25 M) compared to NaCl (0.25 M) provided a maximum separation factor of 1.9 for sodium glucose (0.1 M)/sodium lactate (0.1 M) solutions whereas the separation with NaCl (0.25 M) provided separation factors up to 1.5 and the separation was impossible without the addition of salt.

Modelling of ion rejection in NF is very useful for the optimization and scale-up of water treatment processes, and enormous effort on this field has been expended in the last decades. Ion transport through NF membranes has been widely described by either the non-equilibrium thermodynamic model and its modifications [15–18] or the extended Nernst–Planck equations [19–22].

Among the former, the Spiegler–Kedem (SK) model [15] considered the solute transport as a superposition of (partially uncoupled) convective and diffusive solute flows. In order to include the interactions of solute-solvent, solute-membrane and solvent-membrane, the SK equation was accordingly modified taking into account the influence of membrane structural parameters [23,24] when electrolytes mixtures were employed and the concentration dependence [25] of the

phenomenological transport coefficients using single NaCl and NaBr salts. Then, the number of fitting parameters had to be increased up to six [26]. It was shown how the permeance coefficients to water and solutes can be derived from experimental data and how to choose suitable electroneutrality conditions to obtain the membrane permeances.

Simultaneously, considering up to three ion exclusion mechanisms, i.e. steric, electric (Donnan equilibrium) [27–29] and dielectric - [30–33] exclusion mechanisms and the description of the solute transport in the membrane phase by the extended Nernst-Planck (NP) equation, several parameters of the membrane (such as pore size, fixed charge and dielectric properties) and the ion involved were determined. In addition, several extensions of the NP equations included macroscopic hydrodynamic and electrostatic equations to describe the equilibrium, partitioning and transport of the ions through a nano-porous membrane phase. The use of these complex equations required a large number of fitting parameters that makes difficult the solution of the inverse problem of unambiguous determination of these from experimental data.

An alternative approach is the use of solution-diffusion (SD) model, widely applied originally in RO [34–38]. Unlike the established extended NP or Donnan-Steric-Pore-Dielectric model, the SD model can explain the high SO_4^{2-}/Cl^- selectivity in NF and is in agreement with the weak convective coupling between the solute and solvent transfers in the membrane phase [18,24,39,40]. Yaroshchuk et al. [39] demonstrated that for single salts, the same simple version of SD model coupled with the film model theory, the solution-diffusion-film model (SDF) is applicable. However, for electrolyte mixtures the SDF model had to be extended in order to include the coupling between the electro-diffusion fluxes of various ions via the electric field of membrane potential [41–43]. Taking it into account, a good description of ion rejection dependence on the transmembrane volume flow for a number of electrolyte mixtures could be achieved [41,42]. This approach also accounts for the existence of a concentration-polarization layer where the ion transfer occurs via electro-diffusion as well as via convection due to the solvent transfer. This new description of transmembrane mass transfer by the so-called Solution-Electro-Diffusion-Film (SEDF) model allows for the development of efficient procedures of determination of membrane permeances towards not only salts (P_s) but also single ions (P_i) from experimental data.

The main objective of this work was to extend the validation of the SEDF model via comparing experimental and theoretical data on the rejection of several dominant salts and trace ions using the NF270 membrane in a cross-flow experimental set-up. Synthetic aqueous solutions representative of natural waters influenced by industrial and mining drainage (Na^+, K^+, Mg^{2+}, Cl^-, Br^-, I^-) and industrial wastewaters (NH_4^+, NO_3^-, SO_4^{2-}) were used. Three representative dominant electrolyte types were used ((NaCl (+1:-1), $MgCl_2$(+2,-1), $MgSO_4$(+2,-2)). The membrane permeances with respect to several ions (Na^+, K^+, Cl^-, Ca^{2+}, Mg^{2+}, SO_4^{2-}, NO_3^-, NH_4^+, I^- and Br^-) was calculated.

2. MATERIALS AND METHODS

2.1. Membrane cross-flow set-up

Experiments were performed with a NF270 membrane in a cross-flow set-up equipped with a test cell (GE SEPA^{TM} CF II) with a spacer-filled feed channel and the possibility of independent variation of cross-flow velocity (cfv) and transmembrane pressure (TMP) [42,44]. The membrane area was 0.014 m^2. Feed solutions were kept at constant temperature (23 ± 2ºC) in a thermostated feed tank (30 L) and pumped into the cross-flow filtration system with a high-pressure diaphragm pump (Hydra-Cell, USA) at a prefixed flow rate and pressure. The two output streams from the test cell, permeate and concentrate, were recirculated into the feed tank providing thus a fairly constant concentration in the feed solution. The cfv was fixed and the TMP was varied by a needle valve located in the concentrate stream just at the exit from the test cell. The system was equipped with flow-meters, pressure-meters, a conductivity cell, a pH-meter and a temperature sensor to monitor the hydrodynamic and chemical parameters. Furthermore, a data acquisition system programmed in Labview was developed to ensure the robustness of the system and obtain reproducible data. Sensor calibration was performed under the hydrodynamic conditions used in the experimental work.

2.2. Ion rejection experimental tests of multi-ion electrolyte solutions

Several multi-ion aqueous solutions consisting of a dominant single salt (NaCl, MgCl$_2$ or MgSO$_4$) mixed with trace ions such as Na$^+$, Cl$^-$, Ca^{2+}, Mg^{2+}, SO$_4^{2-}$, K$^+$, NO$_3^-$, NH$_4^+$, I$^-$ and Br$^-$ were used as feed solutions. Common scenarios of low-quality surface waters influenced by industrial and mining drainage containing KCl, MgCl$_2$, KI, NaBr, etc and industrial wastewater containing NH$_4^+$, NO$_3^-$, SO$_4^{2-}$ [45,46] were reproduced by these selected model systems. Before performing any rejection experiments, membranes were wetted overnight in distilled water to wash-out potential storage products. Then, they were compacted with distilled water for one hour and with the working solution over one hour and a half at the maximum working cfv and TMP to ensure constant transmembrane flux in all the experiments at the same pressure requirements. The experimental tests were carried out at a fixed cfv of 0.7 m s^{-1} and the TMP was varied between osmotic pressure of feed solution (4.5-7 bar) and 20 bar. Concentrations of dominant salts in feed solutions were maintained at 10^{-1} mol L^{-1} while concentrations of trace ions were at about 0.5-2% of dominant salt concentrations. All reagents were of analysis quality (PA-ACS-ISO reagent, PANREAC). The conditions of rejection experiments performed with multi-ion solutions are summarized in Table 1.

Table 1. Experimental conditions for the filtration of multi-ion solutions of Na$^+$, Cl$^-$, K$^+$, Ca^{2+}, Mg^{2+}, SO$_4^{2-}$, NO$_3^-$, NH$_4^+$, I$^-$ and Br$^-$ by the NF270 membrane.

| Dominant salts | Trace salt | Feed concentration | | Cross-flow rate | Trans-membrane pressure |
| | | Dominant salt | Trace salt | | |
		$(mol\ L^{-1})$	$(mol\ L^{-1})$	$(m\ s^{-1})$	(bar)
NaCl	$MgSO_4$	10^{-1}	$2 \cdot 10^{-3}$	0.7	4.5 - 20
NaCl	$MgCl_2$	10^{-1}	$2 \cdot 10^{-3}$	0.7	4.5 - 20
NaCl	$CaCl_2$	10^{-1}	$2 \cdot 10^{-3}$	0.7	4.5 - 20
NaCl	KCl	10^{-1}	$2 \cdot 10^{-3}$	0.7	4.5 - 20
NaCl	NH_4Cl	10^{-1}	$2 \cdot 10^{-3}$	0.7	4.5 - 20
NaCl	$NaNO_3$	10^{-1}	$2 \cdot 10^{-3}$	0.7	4.5 - 20
NaCl	NaBr	10^{-1}	$2 \cdot 10^{-3}$	0.7	4.5 - 20
NaCl	NaI	10^{-1}	$2 \cdot 10^{-3}$	0.7	4.5 - 20
$MgCl_2$	KCl	10^{-1}	$5 \cdot 10^{-4}$	0.7	7 - 20
$MgCl_2$	NH_4Cl	10^{-1}	$5 \cdot 10^{-4}$	0.7	7 - 20
$MgCl_2$	Na_2SO_4	10^{-1}	$5 \cdot 10^{-4}$	0.7	7 - 20
$MgCl_2$	$NaNO_3$	10^{-1}	$5 \cdot 10^{-4}$	0.7	7 - 20
$MgCl_2$	NaBr	10^{-1}	$5 \cdot 10^{-4}$	0.7	7 - 20
$MgCl_2$	NaI	10^{-1}	$5 \cdot 10^{-4}$	0.7	7 - 20
$MgSO_4$	NaCl	10^{-1}	$5 \cdot 10^{-4}$	0.7	4.5 - 20
$MgSO_4$	NH_4Cl	10^{-1}	$5 \cdot 10^{-4}$	0.7	4.5 - 20
$MgSO_4$	$NaNO_3$	10^{-1}	$5 \cdot 10^{-4}$	0.7	4.5 - 20
$MgSO_4$	NaBr	10^{-1}	$5 \cdot 10^{-4}$	0.7	4.5 - 20
$MgSO_4$	NaI	10^{-1}	$5 \cdot 10^{-4}$	0.7	4.5 - 20

The transmembrane volume flow (J_v) was determined via monitoring collected permeate volume. Ion concentrations in feed and permeate samples were measured by ion chromatography (Dionex ICS-1000). The cation and anion analyses were performed by using the IONPAC® CS16 cation-exchange column, which uses $3 \cdot 10^{-2}$ mol L^{-1} methane sulphonic acid eluent and the IONPAC® AS23 anion-exchange column. A mixture of $4.5 \cdot 10^{-3}$ mol L^{-1} Na_2CO_3 and $8 \cdot 10^{-4}$ mol L^{-1} $NaHCO_3$ was used as eluent in the latter case. The pH of the feed and permeate solutions were measured with a pH electrode. Overall, in the experimental tests, pH ranged between 5.1 and 6.3.

2.3.   Modelling of ion transfer across NF membranes in multi-ion solutions

In this study, the SEDF model was used to fit experimental data for both dominant and trace ions [41]. The model equations, summarized in Table 2 relates the observable rejections of the dominant salt (R_s^{obs}) and the trace ions (R_t^{obs}) with the corresponding intrinsic ones (R_s^{int} , R_t^{int}) taking into account the concentration polarization and using the unstirred-layer thickness (δ) as

one of the fitting parameters. [41,42],

In order to fit the dominant salt rejections as a function of transmembrane volume flow, two parameters need to be obtained for the dominant salt (by using Eq 8): the membrane and the concentration-polarization layer permeances to the dominant salt (P_s, $P_s^{(\delta)}$). The intrinsic rejection of the dominant salt (R_s^{int}) can then be calculated by Eq. (9) and, then, its reciprocal intrinsic transmission (f_s) and the corresponding membrane surface concentration ($C_s^{(m)}$) can be determined. Once the trace-ion concentrations at the membrane surface are calculated by using Eq. (10), the intrinsic rejections (R_t^{int}) and the corresponding reciprocal transmissions of the trace ions (f_t) can be obtained. Subsequently, in the case of trace ions different from the dominant ions, two parameters, b and K are fitted to Eq 11 and 12. From them, the membrane permeances to dominant and trace ions ($P_\pm$, $P_s^{(\delta)}$) can be calculated with Eq. (13) and the K parameter from Eq. (11), respectively.

Table 2. Summary of mass transport equations of the Solution-Electro-Diffusion-Film (SEDF) model [39,41,42]

$R_s^{obs} \equiv 1 - \dfrac{c_s'}{c_s''}$	(1)
$R_t^{obs} \equiv 1 - \dfrac{c_t'}{c_t''}$	(2)
$R_s^{int} \equiv 1 - \dfrac{c_s'}{c_s^{(m)}}$	(3)
$R_t^{int} \equiv 1 - \dfrac{c_t'}{c_t^{(m)}}$	(4)
$\left(\delta = \dfrac{D_s^{(\delta)}}{P_s^{(\delta)}} \right)$	(5)
$\left(f_s \equiv \dfrac{c_s^{(m)}}{c_s'} \equiv \dfrac{1}{1-R_s^{int}} \right)$	(6)
$\left(f_t \equiv \dfrac{c_t^{(m)}}{c_t'} \equiv \dfrac{1}{1-R_t^{int}} \right)$	(7)

Observable salt rejections

$$R_s^{obs} = \frac{\frac{J_v}{P_s} exp\left(-\frac{J_v}{P_s^{(\delta)}}\right)}{1+\frac{J_v}{P_s} exp\left(-\frac{J_v}{P_s^{(\delta)}}\right)} \quad \text{where } P_s^{(\delta)} = \frac{D_s^{(\delta)}}{\delta}, \; D_s^{(\delta)} = \frac{(Z_+ - Z_-)D_+^{(\delta)}D_-^{(\delta)}}{Z_+D_+^{(\delta)} - Z_-D_-^{(\delta)}} \text{ and } P_s = \frac{D_s}{b} \tag{8}$$

Intrinsic salt rejections

$$R_s^{int} = \frac{\frac{J_v}{P_s}}{1+\frac{J_v}{P_s}} \tag{9}$$

Trace ion concentration at the membrane surface

6

$$\frac{c_t^{(m)}}{c_t^i} = exp(Pe_t)[1 + R_s^{obs}(exp(Pe_s) - 1)]^{b^{(\delta)}} \cdot \left\{ 1 - (1 - R_t^{obs}) \int_{exp(-Pe_t)}^{1} \frac{dy}{[1 + R_s^{obs}(y-\alpha-1)]^{b^{(\delta)}}} \right\}$$

(10)

where $Pe_s = \frac{J_v \cdot \delta}{D_s^{(\delta)}}$, $Pe_t = \frac{J_v \cdot \delta}{D_t^{(\delta)}}$, $b^\delta \equiv \frac{Z_t \cdot (D_+^{(\delta)} - D_-^{(\delta)})}{Z_+ D_+^{(\delta)} - Z_- D_-^{(\delta)}}$, $\alpha = \frac{D_t^{(\delta)}}{D_s^{(\delta)}}$

Reciprocal transmission of trace ion

$$f_t = (f_s)^b + K \cdot \left(\frac{f_s - (f_s)^b}{1-b} \right) \text{ where } f_s = \left(\frac{1}{1 - R_s^{int}} \right), \ f_t = \left(\frac{1}{1 - R_t^{int}} \right), \ b \equiv \frac{Z_t \cdot (P_+ - P_-)}{Z_+ P_+ - Z_- P_-} \text{ and } K \equiv \frac{P_s}{P_t}$$

(11)

Membrane permeances to dominant ions

(12)

$$P_\pm = \frac{P_s}{1 - \left(\frac{Z_+}{P_t} \right) \cdot b}$$

(13)

2.5 NF270 properties

NF270 (Dow Chemical) membrane was used to perform the experimental tests. Its active layer is made of semi-aromatic poly(piperazine) amide whose chemical structure is shown in Figure 1.
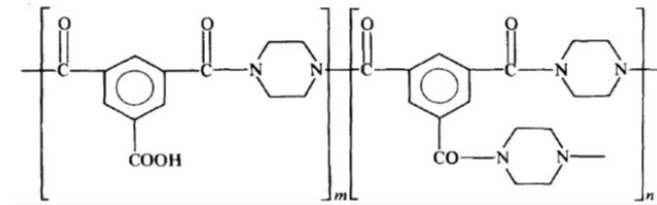
Figure 1. Chemical polymeric structure of NF270 [10,47,48]

Salt and ion permeances can be expected to correlate with the total dominant salt content in the membrane and with changes in the membrane effective fixed charge. The latter can be related to specific ion adsorption and competitive complexing of counter-ions to the fixed charge sites of the polymer membrane matrix, which diminishes the effective fixed charge. Recently aromatic polyamide active layers prepared via interfacial polymerization (similarly to NF270) were characterized in terms of concentration of ionizable functional groups (carboxylic (RCOOH/R-COO-) and amine (R-NH$_3^+$/R-NH$_2$)) related to the degree of polymer cross-linking [7,49]. In the case of NF270, although no data on the acidity constants of the carboxylic groups have been published, most of the characterization studies observed that at neutral pH values 6-7, carboxylic groups are deprotonated (R-COO-). Thus, in the present study where the experiments were performed at pH around 6.6 the carboxylic groups were supposedly deprotonated (R-COO$^-$). Ionizable functional groups can affect water and solute permeation not only because they produce pH-dependent charges in the active layer, but also because they can affect the active layer structure [11].

3. RESULTS AND DISCUSSION

3.1 NaCl as dominant salt

Figure 2 shows the observable rejection for the dominant salt (NaCl) in the presence of a trace salt (referred to as NaCl_CA, where CA is the trace salt) (Fig 2a) and for the trace ions (referred to as C^+ (NaCl_CA) for the cations and A^- (NaCl_CA) for the anions) (Fig 2b) as a function of transmembrane volume flow. The symbols represent the experimental points and the lines were derived by using the SEDF model equations (Table 2). Calculated membrane permeances to dominant and trace ions are collected in Table 3.
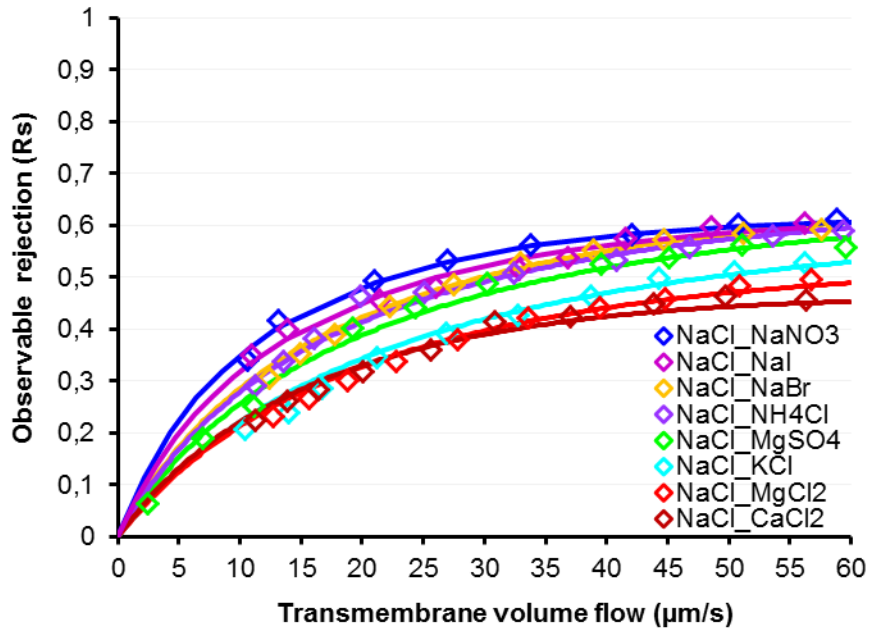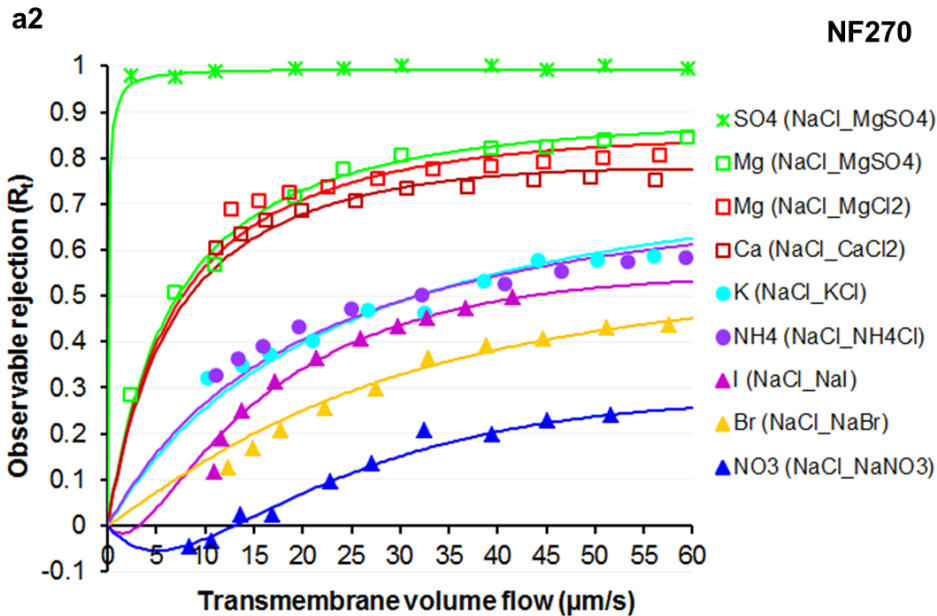
Figure 2. Observable rejections for the dominant salt NaCl in the presence of trace ions (Fig 2a) and for the trace ions (Mg^{2+}, Ca^{2+}, K^+, NH_4^+, SO_4^{2-}, NO_3^-, Br^-, I^-) accompanying the dominant salt (Fig 2b) as a function of transmembrane volume flow. Lines were obtained by the SEDF model.

Table 3. Concentration-polarization layer and membrane permeances to the dominant salt

1 $\left(P_s^{(\delta)}, P_s,\ \text{respectively}\right)$ as well as ionic membrane permeances $\left(P_{\pm}, P_{\pm i}\right)$ of Na⁺, Cl⁻, K⁺, Ca²⁺,

2 Mg²⁺, SO₄²⁻, NO₃⁻, Br⁻, I⁻ and NH₄⁺ from NaCl, MgCl₂ and MgSO₄ based multi-ion solutions by

3 using NF270 membrane.

4

Dominant and trace salts	Salt permeance (µm s⁻¹)		Ion membrane permeance (µm s⁻¹)									
	$P_s^{(\delta)}$	P_s	$P_{NH_4^+}$	P_{K^+}	P_{Na^+}	$P_{Mg^{2+}}$	$P_{Ca^{2+}}$	P_{Cl^-}	P_{Br^-}	$P_{NO_3^-}$	P_{I^-}	$P_{SO_4^{2-}}$
NaCl MgSO₄	119	27	-	-	106	12	-	15	-	-	-	0.09
NaCl MgCl₂	94	33	-	-	662	13	-	17	-	-	-	-
NaCl CaCl₂	69	30	-	-	203	-	14	16	-	-	-	-
NaCl KCl	120	32	-	202	3236	-	-	16	-	-	-	-
NaCl NH₄Cl	110	24	2358	-	298	-	-	12	-	-	-	-
NaCl NaI	65	15	-	-	96	-	-	10	-	-	9	-
NaCl NaBr	112	23	-	-	151	-	-	12	19	-	-	-
NaCl NaNO₃	65	12	-	-	1242	-	-	11	-	18	-	-

Dominant and trace salts	Salt permeance (µm s⁻¹)		Ion membrane permeance (µm s⁻¹)									
	$P_s^{(\delta)}$	P_s	$P_{NH_4^+}$	P_{K^+}	P_{Na^+}	$P_{Mg^{2+}}$	$P_{Ca^{2+}}$	P_{Cl^-}	P_{Br^-}	$P_{NO_3^-}$	P_{I^-}	$P_{SO_4^{2-}}$
MgCl₂ Na₂SO₄	40	2.1	-	-	2116	0.8	-	18	-	-	-	0.9
MgCl₂ KCl	38	2.1	-	99	-	0.8	-	9	-	-	-	-
MgCl₂ NH₄Cl	45	2.1	427	-	-	0.8	-	21	-	-	-	-
MgCl₂ NaI	50	1.8	-	-	27	0.8	-	10	-	-	12	-
MgCl₂ NaBr	47	2.8	-	-	63	1.1	-	14	17	-	-	-
MgCl₂ NaNO₃	38	2.2	-	-	2177	1.0	-	10	-	5	-	-

| Dominant and trace salts	Salt permeance (µm s⁻¹)		Ion membrane permeance (µm s⁻¹)									
	$P_s^{(\delta)}$	P_s	$P_{NH_4^+}$	P_{Na^+}	$P_{Mg^{2+}}$	$P_{Ca^{2+}}$	P_{Cl^-}	P_{Br^-}	$P_{NO_3^-}$	P_{I^-}	$P_{SO_4^{2-}}$	
MgSO₄ NaCl	27	0.1	-	769	1	-	13	-	-	-	0.04	
MgSO₄ NH₄Cl	22	0.2	54	-	2	-	9	-	-	-	0.1	
MgSO₄ NaI	21	0.1	-	50	1	-	-	-	-	19	0.03	
MgSO₄ NaBr	25	0.6	-	57	5	-	-	26	-	-	0.3	
MgSO₄ NaNO₃	23	0.2	-	62	5	-	-	-	41	-	0.1	

For NF270, the rejections of the dominant salt varied between 50-60% (Figure 2a). Trace ions exhibited different selectivity patterns clearly depending on feed solution composition. It is a priori uncertain which of the ions, cations (C^{n+}) or anions (A^{n-}), would be the faster. The electrostatic potential gradient located between both sides of membrane, results in an electric field that accelerates or slows down the ions across the membrane, and concentrates them on both feed and permeate interfaces depending on their own ion charge. Double-charged trace ions (SO_4^{2-}, Mg^{2+}, Ca^{2+}), were mostly better rejected than the dominant salt (NaCl) itself and the single-charged trace ions (Figure 2b). Particularly, the double-charged anion SO_4^{2-} was the best rejected trace ion, exhibiting a percentage removal >98% over the whole range of transmembrane volume flows tested, followed by the double-charged cations Mg^{2+} and Ca^{2+} (with rejection percentages of 80-85% and 75% at the highest flows tested, respectively). This finding is consistent with the fact that the experiments were performed at pH around 6.6±0.2, whereby the carboxylic groups of the polyamide membrane were assumed to be deprotonated (R-COO$^-$) so the permeance to C^{n+} was expected to be significantly higher than that to A^{n-}.

With regards to single-charged trace ions, cations (K^+ and NH_4^+) were better rejected than anions (I^-, Br^-, NO_3^-) just in opposite way of double-charged trace ions (Figure 2b). Although, K^+ and NH_4^+ rejections showed both a very similar pattern increased up to 60%, anions were rejected up to 50% (for I^-), 45% (Br^-) and 20% (NO_3^-) at largest transmembrane volume flows. Besides that, negative rejections of NO_3^- (-5%) were observed at smallest transmembrane volume flow (Figure 2b). Indeed, NO_3^- was more quickly transported to the permeate than Cl^- as their ion membrane permeances values shows (Table 4).

3.2 MgCl$_2$ as the dominant salt

The observable rejection of the dominant salt MgCl$_2$ and the trace ions over the transmembrane volume flows are shown in Figure 3a and Figure 3b respectively, and following the notation described above in section 3.1. Experimental data are represented with symbols whereas their modelling by the SEDF model is shown by lines. The calculated membrane permeances towards the dominants salt and the trace ions by the SEDF model are presented also in Table 3.
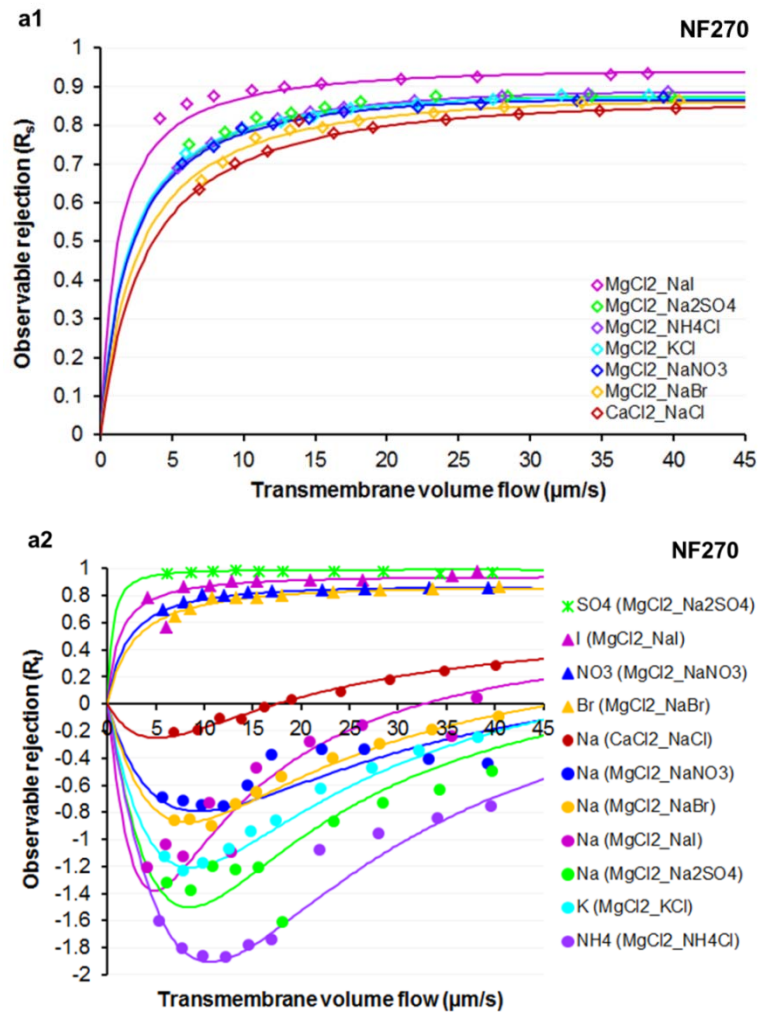
Figure 3. Observable rejections for the dominant salt $MgCl_2$ in the presence of trace ions (Fig 3a) and for the trace ions (Na^+, K^+, NH_4^+, SO_4^{2-}, NO_3^-, Br^-, I^-) accompanying the dominant salt (Fig 3b) as a function of transmembrane volume flow. Lines were obtained by the SEDF model.

It can be observed that the dominant salt and the trace anions were very highly rejected (with removal percentages between 60% and 100%) (Fig 3a and 3b) while the trace cations were poorly rejected showing even negative values (with removal percentages between (-10 % and -190 %) almost over all transmembrane volume flows (Figure 3b).

Compared to NaCl-dominant salt, dominant $MgCl_2$ exhibited higher rejections (85-95%) at the highest transmembrane volume flow (Figure 3a). Similarly to the dominant salt $MgCl_2$, high rejections were also observed for double-charged (SO_4^{2-}) and single-charged (I^-, NO_3^-, Br^-) trace anions (97-99 %and between 85-95 %, respectively, from intermediate to largest transmembrane volume flows). On the other hand, single-charged trace cations exhibited very different rejection patterns, with most of them showing negative rejections over the whole transmembrane volume flows (Figure 3b). The observed rejections at maximum transmembrane volume flows were mostly in the range of -55 % and 5 % for Na^+ (depending upon the trace salt employed), -25% for K^+ and -75% for NH_4^+. At lower transmembrane volume flows, these ions exhibited even lower

11

1 (i.e. more negative) rejection values, with minima at -20% for Na^+ at a transmembrane volume

2 flow of 7 μm/s or -190% for NH_4^+ at a transmembrane volume flow of 12 μm/s). Although, the

3 highest negative rejections of K^+ and NH_4^+ being -125% and -190% respectively and Na^+ with

4 SO_4^{2-} as a counter-ion -150%.$^+$.

5 To sum up, the negative rejection (i.e. permeance through the NF270 membrane) of the positive

6 single-charged trace ions appeared to follow the sequence (in decreasing order) : NH_4^+ >

7 $Na^+(Na_2SO_4)$ > $Na^+(NaI)$ ~ $K^+(KCl)$ > $Na^+(NaBr)$ ~ $Na^+(NaNO_3)$ inversely in accordance with the

8 positive rejection sequence of their electrolyte counter-ions which was SO_4^{2-} > I^- > Br^- ~ NO_3^-

9 (Figure 3b). This finding confirmed that both positive and negative trace ions rejections were

10 strongly controlled by the same magnitude of the electric field that spontaneously arose

11 depending on all involved ions in each experimental test.

12 Results showed that a NF membrane containing negative charged functional groups (carboxylic

13 groups) at the working solution pH, the substitution of the dominant salt from NaCl to $MgCl_2$

14 promotes the possibility to remove from the treated solutions all the mono-charged trace cations

15 (Na^+, K^+, NH_4^+) present in solution (rejections below 0% along the pressure range evaluated).

16

17 **3.3 $MgSO_4$ as dominant salt**

18 Figure 4 shows the observable rejection for the dominant salt $MgSO_4$ in presence of different

19 trace salts (CA) (Fig 4a) and for trace ions (Fig 4b) as a function of the transmembrane volume

20 flow and following the notation described above in section 3.1. The symbols represent the

21 experimental points and the lines were derived by the SEDF model. The calculated membrane

22 permeances to dominant and trace ions are collected in Table 4.
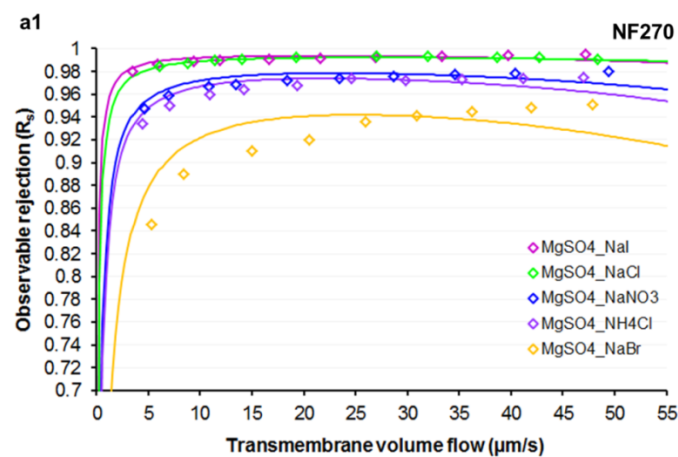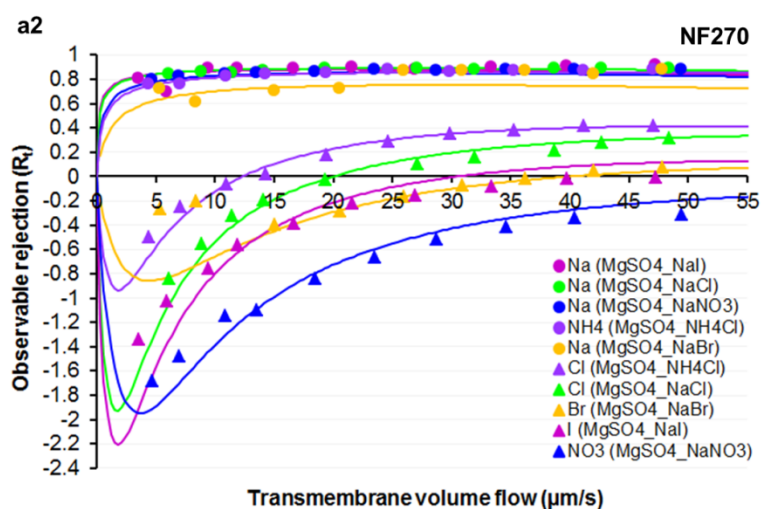

23

Figure 4. Observable rejections for the dominant salt $MgSO_4$ in the presence of trace ions (Fig 4a) and for the trace ions (Na^+, NH_4^+, Cl^-, NO_3^-, Br^-, I^-) accompanying the dominant salt (Fig 4b) as a function of transmembrane volume flow. Lines were obtained by the SEDF model.

When $MgSO_4$ dominant-based solutions were treated by NF270 membrane, both the dominant $MgSO_4$ (Figure 4a) and the single-charged trace cations (Na^+ and NH_4^+) (Figure 4b) were fairly well-rejected over all transmembrane volume flows (with rejection ranges of 85-99 % and 70-90 %, respectively). The rejection of Na^+ and NH_4^+ trace ions seemed little influenced by their counter-ions, showing a subtle rejection sequence depending on their counter-anions as follows: Na^+(NaI) > Na^+(NaCl) > Na^+(NaNO$_3$) > NH_4^+(NH$_4$Cl) > Na^+(NaBr) being in accordance with the dominant salt rejection sequence obtained $MgSO_4$(NaI)≈ $MgSO_4$(NaCl) > $MgSO_4$(NaNO$_3$) ≈ $MgSO_4$(NH$_4$Cl) > $MgSO_4$(NaBr), that was also dependent on the anions from the trace salts.

On the other hand, the single-charged trace anions were poorly rejected showing a wide range on their rejections [-170 to 40 %] including negative values over all transmembrane volume flows (Figure 4b). At the highest transmembrane volume flow, Cl^- was the most rejected regardless the form in which it was added (40% and 30% when it was added as NH$_4$Cl and NaCl, respectively), followed by Br^- and I- (with rejection values lower than 10%) and finally NO_3^-, which was negatively rejected over all transmembrane volume flows. At low transmembrane volume flow, the highest negative rejections of the single-charged anion patterns were determined as the retention sequence follows: Cl^- (-50% (NH$_4$Cl)) < Br^- (-65%) < Cl^- (-84% (NaCl)) < I^- (-135%) < NO_3^- (-168%). This sequence was similarly to that achieved at highest transmembrane volume flows.

As described by Umpuch et al. [14] the separation factor of mixtures of lactate /glucose was achieved by addition of strong electrolytes (Na$_2$SO$_4$ or NaCl) taking benefit of both the power of the dielectric exclusion and the nature of the dominant ions. Then, for example trace cations (organic or inorganic) could be removed from an aqueous solution with a membrane having negatively charged functional groups at the pH of the treated solution by using for example a (+2/-1) type electrolyte (e.g. MgCl$_2$, CaCl$_2$ or BaCl$_2$) promoting the permeation of all cations as the

13

dominant cation (Mg, Ca or Ba) would be highly rejected. Figure 3, shows that the use of a 0.1 M MgCl$_2$ solution provides a 100% removal of Na$^+$ /K $^+$/NH$_4^+$ ions. If the desired objective is to remove anions, a (+2/-2) type electrolyte (e.g. MgSO$_4$) could be used. In Figure 2, permeation values for halides and NO$_3^-$ were below 10%, and separation factors close to 1.5 would be achieved

3.4 Membrane permeances to dominant salt and trace ions: dependence on electrolyte type

The difference in the rejections of the dominant and the trace ions lies on the membrane permeances towards them, which have been calculated by means of the SEDF model as summarized in Table 2. Salt membrane permeances decreased from the highest value 20-30 µm/s measured for NaCl (an electrolyte with two mono-charged species (1:1,Na$^+$/Cl$^-$)) to 1.8-2.8 µm/s for MgCl$_2$ (an electrolyte with one two mono-charged and two double-charged species (2:1,Mg^{+2}/Cl$^-$)) and down to 0.1-0.6 µm/s for MgSO$_4$ (an electrolyte with two double mono-charged species (1:1,Mg^{2+}, SO$_4^{2-}$)).

Among the different mechanisms used for describing ion rejections by NF membranes, the dielectric exclusion mechanism explains the permeance values measured in this study. Yaroshchuk et al. [50] postulated dielectric exclusion as one of separation mechanisms of NF. Dielectric exclusion is caused by the interactions of ions with the bound electric charges induced by ions at interfaces between media of different dielectric constants (e.g. carboxylic and amine groups of NF270). The dielectric exclusion from the polymer network pores of the membranes with closed geometry is shown to be essentially stronger than that from free volume with relatively open geometry. Originally it was common to believe that their main rejection mechanism was the Donnan exclusion caused by a fixed electric charge. That conclusion was based, in fact, on the only observation that double-charge anions were rejected essentially better than single-charge ones. However, that is characteristic of dielectric exclusion too. According to Kim et al. [49] thin film polyamide layers of RO and NF membranes have a bimodal distribution with sizes (e.g 2.1-2.4 Å and 3.5-4.5 Å for FT30 RO membrane), which is just the range where the dielectric exclusion can be strong. In principle, that mechanism is more universal than the Donnan exclusion because a membrane may have or may not have a fixed charge (e.g. NF270 as a function of the pH), however, the existence of a low dielectric constant matrix is beyond any doubt.

Thus, due to the dielectric exclusion membranes protect themselves from the intrusion of ions which gives rise to the screening of dielectric exclusion itself. Both mechanisms, the dielectric and Donnan exclusions, cause a rejection of ions. However, they are far from being simply additive, and the interaction between them is non-trivial. Indeed, it has been shown that a fixed charge

makes the screening of interactions with polarization charges stronger thus making the dielectric exclusion weaker [50,51]. At the same time the dielectric exclusion is equivalent to a decrease in the bulk electrolyte concentration. The latter is known to cause an increase in the Donnan exclusion. Thus, the dielectric exclusion makes the Donnan exclusion stronger, whereas the presence of fixed charge makes the dielectric exclusion weaker. That can be illustrated by the effect of dielectric exclusion on the relationship between fixed charge density and Donnan potential. It essentially depends on the pore geometry parameter and the type of electrolyte according to the ions valance.

For instance, for 1:1 (e.g. NaCl) electrolytes dielectric exclusion is lower than for electrolytes with double-charge counter-ions 2:1 (e.g. $MgCl_2$), which in turn is lower than for electrolytes containing double-charge ions (2:2) ($MgSO_4$). Therefore in the case of electrolytes with double-charge counter-ions such as $MgSO_4$ a fixed charge of considerable magnitude is likely to cause a decrease in reflection coefficient. At the same time a fixed charge of moderate magnitude may be beneficial for membrane performance. This behavior has been extended to other electrolytes data for NF270 reported in the literature and the same trend is reported, as it is the case of $CaCl_2$ and Na_2SO_4 with permeance values of 4.8-5 µm/s, and 0.1-0.2 µm/s, respectively [42,52].

A second phenomenon related to the presence of charges on the membrane structure should be stressed. As discussed above, the isoelectric point at the solution pH, the free carboxylic groups are ionized. Then, for a given electrolyte, the negative ion (e.g. Cl^- in NaCl and $MgCl_2$ and SO_4^{-2} in $MgSO_4$), will suffer from electrical repulsion, and then rejected in a stronger way than the positively charged ion (e.g. Na^+ in NaCl or Mg^{+2} in $MgCl_2$ and $MgSO_4$). This is in agreement with the measured ion permeances, where the most potentially fast ion from this couple (Na^+, Mg^{+2}) is expected to be the Na^+. Na^+ has the largest ion permeances >100 for all the experiments with NaCl as dominant salt higher than Mg^{+2}, affected additionally by the dielectric exclusion effect. With regards to anions, the potentially fastest ion was Cl^- with permeance values of 11-17 µm/s for both NaCl and $MgCl_2$ dominant salts, followed by sulfate with permeance values of 0.05-0.1 µm/s for dominant $MgSO_4$, due to the dielectric exclusion effect. Similar values of permeances for SO_4^{2-} were reported by Pages et al. [42] for dominant Na_2SO_4 dominant salt experiments.

The influence of the nature of the dominant electrolyte on the membrane permeance to the trace ions was also extracted from experimental data by using the SEDF model. Results, collected in Table 3, showed that membrane permeances to trace cations (Na^+, Mg^{2+}) were similar as those determined for them in experiments as dominant salt. Then, size exclusion mechanism as it is claiming in some NF models is not having a relevant contribution for Na^+ rejections and solution composition (nature of the dominant electrolyte) and the membrane properties are having a highest contribution.

Membrane permeance values to NH_4^+ were approx. 400 µm/s and 2300 µm/s in NaCl- and $MgCl_2$-dominated solutions, respectively, much higher than the value of 54 µm/s corresponding to a $MgSO_4$-dominated solution. This latter low value is due to the fact that in a solution dominated by

a 2:2 type electrolyte, the negatively charged ion (SO_4^{2-} in this case) accelerates trace anions permeation while des-accelerates the transport of cations such as NH_4^+. The same explanation as before applies to the permeance values to K^+ (approx. 200 µm/s and 100 µm/s for NaCl- and $MgCl_2$-dominated solutions, respectively) are slightly lower than to NH_4^+.

It is of particular mention the behavior of ion permeances of Na^+. For dominant NaCl and $MgCl_2$ solutions Na^+ ion is showing the highest ion permeances with values higher than 100. However in dominant $MgSO_4$ solutions as trace values of rejection measured range from 0 up to –80% at the maximum linear velocity. For the case of anionic species, sulfate ions as trace component in $MgCl_2$ and NaCl, solutions provided permeance values similar to those for dominant salts as well as chloride ions in $MgSO_4$ dominant salt concentration. For the case of non-common anions such as Br^-, I^- and NO_3^-, values reported were similar to a monovalent ion as Cl^-. Both Br^- and I^- have similar chemical properties, although different size properties as it is reported by the hydrated radius with values of 330 pm, and 340 pm respectively, and 195 pm for Cl^-. However this has not been traduced in such different ion permeances as it is claimed by models considering size exclusion effects. Similarly NO_3^- (340 pm hydrated radius), a single charge ion, with also similar permeance values to halide anions.

4. CONCLUSIONS

In order to study the effect of dominant salt concentration on the removal of trace ions (Na^+, K^+, Cl^-, Ca^{2+}, Mg^{2+}, SO_4^{2-}, NO_3^-, NH_4^+, Br^- and I^-) a set of NF experiments with different dominant salts (NaCl, $MgCl_2$, $MgSO_4$) was designed. The rejections of easily-permeating ions such as single-charge inorganic ions in NF membranes containing ionisable free carboxylic and amine groups are controlled to a larger extent by a combination of the electric field, the membrane permeance to them, the membrane properties and the solution composition. The experimental data with various trace ions and dominant salts confirm this hypothesis and can be qualitatively interpreted within the scope of extended SEDF model in the case of feed solutions consisting of one dominant salt and (any number of) trace ions.

The applicability of the SEDF model was confirmed, since it was possible to fit the experimental data by means of the model, even in the case of negative rejections. The successful SEDF model fitting highlighted the importance of the polarization layer and electric-field effects on which the model is based. The study has demonstrated severe changes on the selectivity rejection of inorganic ions as Br^-, I^-, NO_3^-, NH_4^+, K^+ depending on the environment solutions. Although the information on the membrane permeances to ions has remained empirical in this study, in principle, it can further be used for the verification of self-consistency of various mechanistic models. The availability of three "measurable" quantities, the membrane permeances to the cations and anions of the dominant salt as well as to the trace ions, in contrast to just one permeance to the salt available from conventional measurements with single salts, can make self-

1   consistency checks much more conclusive.

2

3   5   ACKNOWLEDGMENTS

11

Nomenc

lature

A	water permeance defined on Eq. (1)
c_i, c_j	ion and water molecules concentrations (mol m^{-3})
c_j'	water molecules concentration in the feed solution (mol m^{-3})
c_s'	salt concentration in the feed solution (mol m^{-3})
$c_s^{(m)}$	salt concentration at the membrane surface (mol m^{-3})
c_s''	salt concentration in the permeate (mol m^{-3})
c_t'	trace ion concentration in the feed solution (mol m^{-3})
$c_t^{(m)}$	trace ion concentration at the membrane surface (mol m^{-3})
c_t''	trace ion concentration in the permeate (mol m^{-3})
D_i, D_j	ion and water molecules diffusion coefficients in the membrane (m^2 s^{-1})
$D_i^{(\delta)}$	solute diffusion coefficient in the concentration-polarization layer (m^2 s^{-1})
$D_+^{(\delta)}$	dominant ion diffusion coefficients in the concentration-polarization layer (m^2 s^{-1})
$D_s^{(\delta)}$	dominant salt diffusion coefficient in the concentration-polarization layer (m^2 s^{-1})
$D_t^{(\delta)}$	trace ion diffusion coefficient in the concentration-polarization layer (m^2 s^{-1})
f_s	reciprocal dominant salt transmembrane transfer
f_t	reciprocal trace ion transmembrane transfer
K_j	liquid-membrane sorption coefficient defined on Eq. (1)
$P_s^{(\delta)}$	concentration-polarization layer permeance to the dominant salt (m s^{-1})
P_s	membrane permeance to the dominant salt (m s^{-1})
$P_\pm$	membrane permeances to the dominant ions (m s^{-1})
P_t	membrane permeances to the trace ions (m s^{-1})
Pe_s	dominant salt Péclet number

Pe_t	trace ion Péclet number
R	gas constant (J K^{-1} mol^{-1})
R_s^{int}	dominant salt intrinsic rejection
R_t^{int}	trace ion intrinsic rejection
R_s^{obs}	dominant salt observable rejection
R_t^{obs}	trace ion observable rejection
T	temperature (K)
v_i	solute molar volume (m^3 mol^{-1})
x	coordinate scaled on the membrane thickness (m)
z_i	ion charge
$z_\pm$	dominant ion charges
z_t	trace ion charge

Greek letters

α	fraction of trace ion over salt diffusion coefficients in the concentration polarization-layer
γ_j^i	activity coefficient of the bulk feed solution
$\gamma_j^{(m)}$	activity coefficient of the feed-membrane interphase
δ	estimated concentration-polarization thickness (m)
φ	dimensionless reference electrostatic potential

REFERENCES

[1]   S. Darvishmanesh, T. Robberecht, P. Luis, J. Degrève, B. Van der Bruggen, Performance of Nanofiltration Membranes for Solvent Purification in the Oil Industry, J. Am. Oil Chem. Soc. 88 (2011) 1255–1261.

[2]   A. Sotto, J.M. Arsuaga, B. Van der Bruggen, Sorption of phenolic compounds on NF/RO membrane surfaces: Influence on membrane performance, Desalination. 309 (2013) 64–73.

[3]   S.K. Nataraj, K.M. Hosamani, T.M. Aminabhavi, Nanofiltration and reverse osmosis thin film composite membrane module for the removal of dye and salts from the simulated mixtures, Desalination. 249 (2009) 12–17.

[4]   B. Van der Bruggen, J. Kim, Nanofiltration of aqueous solutions: Recent developments and progresses, in: Adv. Mater. Membr. Prep., 2012: pp. 228–247.

[5]   O. Coronell, B.J. Mariñas, X. Zhang, D.G. Cahill, Quantification of functional groups in the active layer of nanofiltration (NF) and reverse osmosis (RO) membranes, (2007).

[6]   D.L. Oatley, L. Llenas, R. Pérez, P.M. Williams, X. Martínez-Lladó, M. Rovira, Review of the dielectric properties of nanofiltration membranes and verification of the single oriented layer approximation., Adv. Colloid Interface Sci. 173 (2012) 1–11.

[7]   O. Coronell, M.I. González, B.J. Mariñas, D.G. Cahill, Ionization behavior, stoichiometry of association, and accessibility of functional groups in the active layers of reverse osmosis and nanofiltration membranes., Environ. Sci. Technol. 44 (2010) 6808–6814.

[8]   A.E. Childress, M. Elimelech, Effect of solution chemistry on the surface charge of

18

polymeric reverse osmosis and nanofiltration membranes, J. Memb. Sci. 119 (1996) 253–268.

[9]   L. a. Richards, M. Vuachère, A.I. Schäfer, Impact of pH on the removal of fluoride, nitrate and boron by nanofiltration/reverse osmosis, Desalination. 261 (2010) 331–337.

[10]   E. Idil Mouhoumed, a. Szymczyk, a. Schäfer, L. Paugam, Y.H. La, Physico-chemical characterization of polyamide NF/RO membranes: Insight from streaming current measurements, J. Memb. Sci. 461 (2014) 130–138.

[11]   O. Coronell, B.J. Mariñas, D.G. Cahill, Depth heterogeneity of fully aromatic polyamide active layers in reverse osmosis and nanofiltration membranes., Environ. Sci. Technol. 45 (2011) 4513–20.

[12]   A.I. Schäfer, A.. Fane, T.D. Waite, Nanofiltration of natural organic matter : Removal , fouling and the influence of multivalent ions, Desalination. 118 (1998) 109–122.

[13]   R.S. Harisha, K.M. Hosamani, R.S. Keri, S.K. Nataraj, T.M. Aminabhavi, Arsenic removal from drinking water using thin film composite nanofiltration membrane, Desalination. 252 (2010) 75–80.

[14]   C. Umpuch, S. Galier, S. Kanchanatawee, H.R. Balmann, Nanofiltration as a purification step in production process of organic acids: Selectivity improvement by addition of an inorganic salt, Process Biochem. 45 (2010) 1763–1768.

[15]   K.S. Spiegler, O. Kedem, Thermodynamics of hyperfiltration (reverse osmosis): criteria for efficient membranes, Desalination. 1 (1966) 311–326.

[16]   A.E. Yaroshchuk, Rejection of single salts versus transmembrane volume flow in RO/NF: thermodynamic properties, model of constant coefficients, and its modification, J. Memb. Sci. 198 (2002) 285–297.

[17]   J. Schaep, B. Van der Bruggen, C. Vandecasteele, D. Wilms, Influence of ion size and charge in nanofiltration, Sep. Purif. Technol. 14 (1998) 155–162.

[18]   S. Bason, Y. Kaufman, V. Freger, Analysis of ion transport in nanofiltration using phenomenological coefficients and structural characteristics, J. Phys. Chem. B. 114 (2010) 3510–3517.

[19]   J. Garcia-Aleman, J.M. Dickson, Mathematical modeling of nanofiltration membranes with mixed electrolyte solutions, J. Memb. Sci. 235 (2004) 1–13.

[20]   W.R. Bowen, H. Mukhtar, Characterisation and prediction of separation performance of nanofiltration membranes, J. Memb. Sci. 112 (1996) 263–274.

[21]   W.R. Bowen, J.S. Welfoot, P.M. Williams, Linearized transport model for nanofiltration: Development and assessment, AIChE J. 48 (2002) 760–773.

[22]   D.W. Nielsen, G. Jonsson, Bulk-phase criteria for negative ion rejection in nanofiltration of multicomponent salt solutions, Sep. Sci. Technol. 29 (1994) 1165–1182.

[23]   G. Jonsson, Concentration profiles retention—flux curves for composite membranes in reverse osmosis, J. Memb. Sci. 14 (1983) 211–227.

[24]   J. Jagur-Grodzinski, O. Kedem, Transport coefficients and salt rejection in unchanged hyperfiltration membranes, Desalination. 1 (1966) 327–341.

[25]   S. Bason, O. Kedem, V. Freger, Determination of concentration-dependent transport coefficients in nanofiltration: Experimental evaluation of coefficients, J. Memb. Sci. 326 (2009) 197–204.

[26]   X.L. Wang, Y.Y. Fang, C.H. Tu, B. Van der Bruggen, Modelling of the separation performance and electrokinetic properties of nanofiltration membranes, Int. Rev. Phys. Chem. 31 (2012) 111–130.

[27]   X.-L. Wang, T. Tsuru, S. Nakao, S. Kimura, Electrolyte transport through nanofiltration membranes by the space-charge model and the comparison with Teorell-Meyer-Sievers model, J. Memb. Sci. 103 (1995) 117–133.

[28] M.D. Afonso, M.N. De Pinho, Transport of MgSO4, MgCl2, and Na2SO4 across an amphoteric nanofiltration membrane, J. Memb. Sci. 179 (2000) 137–154.

[29] L. Bruni, S. Bandini, Studies on the role of site-binding and competitive adsorption in determining the charge of nanofiltration membranes, Desalination. 241 (2009) 315–330.

[30] A. Szymczyk, P. Fievet, Investigating transport properties of nanofiltration membranes by means of a steric, electric and dielectric exclusion model, J. Memb. Sci. 252 (2005) 77–88.

[31] a Szymczyk, N. Fatinrouge, P. Fievet, C. Ramseyer, a Vidonne, Identification of dielectric effects in nanofiltration of metallic salts, J. Memb. Sci. 287 (2007) 102–110.

[32] A.A. Hussain, S.K. Nataraj, M.E.E. Abashar, I.S. Al-mutaz, T.M. Aminabhavi, Prediction of physical properties of nanofiltration membranes using experiment and theoretical models, J. Memb. Sci. 310 (2008) 321–336.

[33] N.S. Kotrappanavar, A.A. Hussain, M.E.E. Abashar, I.S. Al-mutaz, T.M. Aminabhavi, M.N. Nadagouda, Prediction of physical properties of nanofiltration membranes for neutral and charged solutes, Desalination. 280 (2011) 174–182.

[34] P.V.X. Hung, S.-H. Cho, S.-H. Moon, Prediction of boron transport through seawater reverse osmosis membranes using solution–diffusion model, Desalination. 247 (2009) 33–44.

[35] A. Bódalo, J.-L. Gómez, E. Gómez, G. León, M. Tejera, Reduction of sulphate content in aqueous solutions by reverse osmosis using cellulose acetate membranes, Desalination. 162 (2004) 55–60.

[36] A. Bódalo, J.-L. Gómez, E. Gómez, G. León, M. Tejera, Ammonium removal from aqueous solutions by reverse osmosis using cellulose acetate membranes, Desalination. 184 (2005) 149–155.

[37] J.G. Wijmans, R.W. Baker, The solution-diffusion model: a review, J. Memb. Sci. 107 (1995) 1–21.

[38] D. Paul, Reformulation of the solution-diffusion theory of reverse osmosis, J. Memb. Sci. 241 (2004) 371–386.

[39] A. Yaroshchuk, X. Martínez-Lladó, L. Llenas, M. Rovira, J. de Pablo, J. Flores, et al., Mechanisms of transfer of ionic solutes through composite polymer nano-filtration membranes in view of their high sulfate/chloride selectivities, Desalin. Water Treat. 6 (2009) 48–53.

[40] V. Sasidhar, E. Ruckenstein, Anomalous effects during electrolyte osmosis across charged porous membranes, J. Colloid Interface Sci. 85 (1982) 332–362.

[41] A. Yaroshchuk, X. Martínez-Lladó, L. Llenas, M. Rovira, J. de Pablo, Solution-diffusion-film model for the description of pressure-driven trans-membrane transfer of electrolyte mixtures: One dominant salt and trace ions, J. Memb. Sci. 368 (2011) 192–201.

[42] N. Pages, A. Yaroshchuk, O. Gibert, J.L. Cortina, Rejection of trace ionic solutes in nanofiltration: Influence of aqueous phase composition, Chem. Eng. Sci. 104 (2013) 1107–1115.

[43] A. Yaroshchuk, M.L. Bruening, E.E. Licón Bernal, Solution-Diffusion–Electro-Migration model and its uses for analysis of nanofiltration, pressure-retarded osmosis and forward osmosis in multi-ionic solutions, J. Memb. Sci. 447 (2013) 463–476.

[44] M. Reig, N. Pagès, E. Licon, C. Valderrama, O. Gibert, A. Yaroshchuk, et al., Evolution of electrolyte mixtures rejection behaviour using nanofiltration membranes under spiral wound and flat-sheet configurations, Desalin. Water Treat. 56 (2014) 3519–3529.

[45] M. Reig, E. Licon, O. Gibert, A. Yaroshchuk, J.L. Cortina, Rejection of ammonium and nitrate from sodium chloride solutions by nanofiltration: Effect of dominant-salt concentration on the trace-ion rejection, Chem. Eng. J. 303 (2016) 401–408.

[46] J. Raich-Montiu, J. Barios, V. Garcia, M.E. Medina, F. Valero, R. Devesa, et al., Integrating membrane technologies and blending options in water production and

distribution systems to improve organoleptic properties. The case of the Barcelona Metropolitan Area, J. Clean. Prod. 69 (2014) 250–259.

[47]   A. Sotto, ARCADIO SOTTO DÍAZ, (2008).

[48]   W.J. Koros, G.K. Fleming, S.M. Jordan, T.H. Kim, H.H. Hoehn, POLYMERIC MEMBRANE MATERIALS SOLUTION-DIFFUSION BASED PERMEATION SEPARATIONS Membrane science and polymer science have grown synergistically over the past thirty years . Clearly , today ' s impressive set of membrane processes and products could not exist, 13 (1988) 339–401.

[49]   S.H. Kim, S.-Y. Kwak, T. Suzuki, Positron annihilation spectroscopic evidence to demonstrate the flux-enhancement mechanism in morphology-controlled thin-film-composite (TFC) membrane., Environ. Sci. Technol. 39 (2005) 1764–70.

[50]   A.E. Yaroshchuk, Dielectric exclusion of ions from membranes, Adv. Colloid Interface Sci. 85 (2000) 193–230.

[51]   S. Bandini, D. Vezzani, Nanofiltration modeling: the role of dielectric exclusion in membrane characterization, Chem. Eng. Sci. 58 (2003) 3303–3326.

[52]   A. Yaroshchuk, X. Martínez-Lladó, L. Llenas, M. Rovira, J. de Pablo, Solution-diffusion-film model for the description of pressure-driven trans-membrane transfer of electrolyte mixtures: One dominant salt and trace ions, J. Memb. Sci. 368 (2011) 192–201.